J. Phys. A: Math. Gen. 28 (1995) 5117–5129. Printed in the UK

# Three-state Potts antiferromagnet on the triangular lattice

J Adler†, A Brandt‡, W Janke§ and S Shmulyian‡

† Department of Physics, Technion—Israel Institute of Technology, Haifa 32000, Israel
‡ Department of Applied Mathematics, Weizmann Institute of Science, Rehovot, 76100, Israel
§ Institut für Physik, Johannes Gutenberg-Universität, 55099 Mainz, Germany

Received 18 May 1995

**Abstract.** The three-state Potts antiferromagnetic model on the triangular lattice (3PAFT) has a weak first-order transition in the pure case. The first-order nature follows from analytic arguments and while it has been observed in some simulations, the precision of (and internal disagreement between) these observations has left much to be desired. The 3PAFT is the only two-dimensional nearest-neighbour Potts model with an ordered phase that does not have an infinite degeneracy, that remains without an exact value for its critical point. This model is expected to exhibit interesting glassy behaviour and a possible crossover to a second-order transition upon dilution. A careful characterization of the nature of the pure transition is needed in order to explore the physics of the dilute model. We find clear indication of a first-order transition at $T_t = 0.627\,31 \pm 0.000\,06$, using a cluster method that can be extended to the dilute case and histogram reweighting analysis. Our estimate is two orders of magnitude more precise than previous simulations and falls within the error bounds of a reanalysis of existing series expansion ($T_t = 0.628 \pm 0.004$) reported on herein.

## 1. Introduction

The three-state Potts model on the triangular lattice (3PAFT) is a very special case among two-dimensional Potts models. Unlike the $q \geqslant 3$ antiferromagnetic models on the square lattice and the $q \geqslant 4$ antiferromagnetic models on the triangular lattice there is no infinite ground-state degeneracy or lack of finite-temperature order, rather a simple set of six ground states (Schick and Griffiths [1]). Early Monte Carlo simulations by Grest [2] and Saito [3] and series expansion combined with heuristic arguments put forward by Enting and Wu [4], indicated that the transition is of first order. Baxter (private communication) has argued that exact considerations imply that this system cannot have a finite temperature second-order transition.

We begin this paper by presenting our motivation for studying this model and for selecting the techniques we have used. We will then review extant numerical studies of both the pure and dilute systems, describe our techniques of both simulation and analysis and present our new results.

Our original motivation for the 3PAFT project was the exploration of several aspects of the (site) dilute 3PAFT system that are of current physical interest. However, study of the dilute model requires careful characterization of the pure transition. In this paper we will only discuss the pure model in detail, but since our eventual aim of studying the dilute model is relevant to the results presented below as justification for selection of the numerical techniques we will make some general comments on the dilute systems. One of the aspects of interest in the dilute model is at small dilution. Here, there might be a crossover to a second-order transition. Such crossovers to second-order transitions occur in related

0305-4470/95/185117+13$19.50  

models such as the dilute Baxter–Wu model (Novotny and Landau [5], Novotny and Evertz [6]), and the second-order transitions in some cases have Ising exponents for reasons not well understood to date. In the Baxter–Wu case it is a crossover between different types of second-order transitions and in the 3PAFT it would be first to second order and thus of interest both intrinsically and as a comparison. To explore the small dilution case a method that enables a high quality characterization of the first-order transition is needed so that we can determine if the first-order transition will extend to the dilute case (contrary to expectations) and if not how the crossover will take place. Hence we chose to use a histogram reweighting approach, which is capable of detecting even weak first-order transitions. The second aspect of interest is at larger dilution where there are long relaxation times and might be some partial order and glassy effects. Here there are applications to systems such as quadrupolar glasses (Reger and Binder [7]). The zero-temperature behaviour of this model was studied by Adler *et al* [8, 9]. Attempts to study the dilute system have been made (Fried [10]), on samples up to $36 \times 36$. They were limited by the long relaxation times and the impossibility of reaching system sizes that might be adequate to probe the long-range connectivity that is an essential part of the partial order, but did suggest that further investigation would be worthwhile. To increase the system size a multiscale (in particular, cluster) approach is desirable. Thus in order to explore both small and large dilution in this model we decided to develop a cluster algorithm combining this with histogram reweighting analysis on the results.

While searching for a study of the pure system to calibrate our new techniques it became clear that we would have to undertake this first ourselves, as the existing studies did not converge to a single estimate with enough significant figures for comparison purposes. Although this was a detour, we did feel that such an apparently simple model should not be the only two-dimensional Potts model without a precise characterization of its phase transition. Thus we have carried out this characterization with extreme care and have added several significant figures to previous estimates. Existing simulations of the first-order transition in the pure system give different results and use very different simulation methods. Before presenting these results, a word about units. We write the Hamiltonian of the 3PAFT model as

$$H = -J \sum_{\langle ij \rangle} \delta_{s_i, s_j} \tag{1.1}$$

with $J < 0$. Many of the previous measurements were made in terms of $J/k_B$, and thus we will use the notation $T_t$ for the transition point in these terms and relate to $u = e^K$, the low-temperature series expansion variable, where needed for comparisons ($K = J/k_BT$ is the high-temperature series expansion variable). By studying the energy and the magnetization Grest [2] observed a first-order transition near $T_t \approx 0.63$ from a $51 \times 51$ lattice. Saito [3] measured a transition temperature of $K_t \approx -1.585$ ($T_t \approx 0.631$) from a $60 \times 60$ lattice, and more recently Ono and De Meo [11] using an interface method obtained $T_t \approx 0.625$ from lattices up to $40 \times 120$. There is also a series expansion study by Enting and Wu [4] who generated short series for the partition function, order parameter and susceptibility in the variable $u$. Strictly speaking, since this is a first-order transition standard Dlog Padé methods should not give the exact transition temperature (Adler and Privman [12]), however, Briggs *et al* [12] (as well as analyses by one of the authors of ferromagnetic large-$q$ Potts models series developed by Schreider and Reger [13]) show that Dlog Padé gives a divergence at some associated singularity that is remarkably close to the exact transition point (agreement of several significant figures being seen for weak first-order transitions.) Enting and Wu quoted $u_t = 0.204 \pm 0.003$ (or $T_t = 0.629 \pm 0.005$) from two analyses and $0.203 \pm 0.002$

(or $T_t = 0.627 \pm 0.004$) from another. In addition to the simulation results we will also report below on a reanalysis of these series using the so-called M1 and M2 methods (Adler *et al* [14]).

## 2. The algorithm

Let us now describe the selection of the algorithm for our simulation which, as explained above, is a cluster method that was designed with eventual application to the dilute system in mind. Although such a cluster method should not be expected to be more efficient for a first-order transition than a simple one we shall show below that it does appear to be somewhat faster here too.

### *2.1. Description*

Several different simulation methods were used in the development phase, including a simple Metropolis and heat bath, as well as different cluster approaches. While developing the latter, we sought for ways to adapt the Swendsen–Wang (SW) [15] type ideology to the 3PAFT framework, which appeared to be non-trivial. In the original SW algorithm, designed for the ferromagnetic Potts model, each lattice bond is, in turn, either 'frozen' or 'deleted', through setting the values of the corresponding coupling constant to infinity or zero, respectively, according to a simple rule which maintains detailed balance with respect to the original Hamiltonian. After similarly treating ('killing') all the bonds, one is left with a number of independent ferromagnetic clusters, allowing for an easy and fast simulation. In the framework of the 3PAFT, however, a naive application of the SW technique would yield clusters of non-regular structure, since the complete (antiferromagnetic) order in this case may not be propagated by means of a single bond. As a solution to this problem, we developed the following cluster algorithm which successfully copes with the order propagation task. In the figure which accompanies the description below the three states of the 3PAFT spins are indicated by the letters A, B and C.

At first, an antiferromagnetic analogue of the SW rule is applied to the lattice bonds in some prescribed order until a particular bond happens to get frozen (near the transition temperature, that typically takes only a few steps). That bond, complete with the sites it spans, comprises a cluster seed. Next, for each of the two sites $\alpha$, coupled to *both* $i$ and $j$ by living bonds ($\alpha \in \{k, l\}$ in figure 1($a$)), the stochastic decision about their *simultaneous* killing is made: both bonds are deleted with probability

$$p_d = \mathrm{e}^{-K(\delta_{s_\alpha,s_i}+\delta_{s_\alpha,s_j}-1)} \tag{2.1}$$

and frozen with probability

$$p_f = 1 - p_d\,. \tag{2.2}$$

Clearly the bond freezing takes place only if the inclusion of the site $\alpha$ in the growing cluster preserves the complete antiferromagnetic order. Newly frozen bonds are further used for similarly enlarging the cluster by means of additional sites (figure 1($b$)), etc. The formation of the cluster terminates at a stage when none of the frozen bonds has a neighbouring site coupled to it by two living interactions (figure 1($c$)). The consequent clusters are

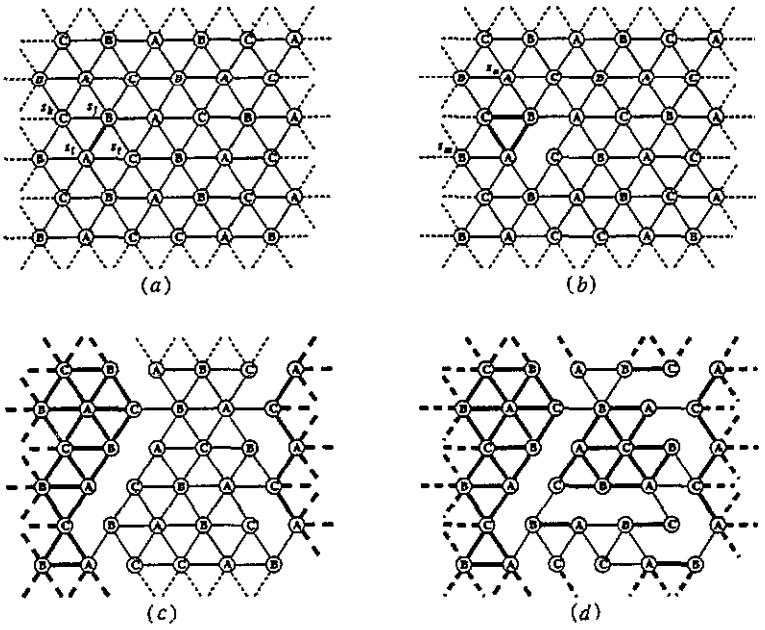


**Figure 1.** Stages of the 2LA coarsening on a $6 \times 6$ lattice: (*a*) processing spins $s_k$ and $s_l$ neighbouring to the seed, (*b*) processing spins $s_m$ and $s_n$ neighbouring to bonds included in the cluster on the previous stage, (*c*) end of the cluster formation, (*d*) end of coarsening. Bold lines denote frozen bonds; deleted bonds are not shown. The letters A, B and C represent the three possible spin states.

constructed, in a similar manner, of sites not contained in the already formed clusters. The procedure continues until no new cluster seed may be chosen (figure 1(*d*)).

At this point, the whole lattice is partitioned into a number of antiferromagnetic clusters usually coupled by quite a few living bonds. In this set-up, each cluster may easily be simulated by choosing one of the six permutations of the spin states within the cluster (corresponding to the six ground states) according to its remaining connections with other clusters. This allows for performing an arbitrary number of Monte Carlo sweeps over all the clusters. Restoring all lattice bonds to their original states completes the iteration of the algorithm.

For the transition temperature simulations, we selected the above algorithm with a single cluster-by-cluster Monte Carlo sweep within each iteration. It appeared that additionally employing single-site sweeps (intended to locally construct a basis for an efficient clustering) was not beneficial, and since implementing just a pure cluster algorithm is computationally more efficient this sufficed. The statistical validity of the algorithm as well as details of the other algorithms are discussed elsewhere in depth (Shmulyian [16]), with a brief outline of the proof of the detailed balance being given below in the appendix.

The algorithm developed may easily be extended to the case of an arbitrary site dilution; the efficiency of the relevant implementation is currently being investigated.

### 2.2. *Survey of preliminary experiments*

The selection process was based in part on insight gained by watching the approach to equilibrium of different algorithms at different temperatures. The motivation of the eventual study of the dilute model also played a role, and we freely admit that we may not have

selected the one and only optimal algorithm but rather one good for our purposes. This was done with interactive visualization (in C with X11 graphics for the algorithm and in FORTRAN with PGPLOT for the analysis routines) based on the ideas proposed by Silverman and Adler [17] (1991) for animated simulated annealing.

At low temperatures the cluster algorithm was clearly superior to a single-site Metropolis. For example, starting from a random $60 \times 60$ configuration at $T = 0.45$ the former algorithm reached the global minimum ground state in less than 200 iterations, whereas the latter always remained in a local minima (multidomain) state even after several thousands of sweeps.

Near the transition slowing down (even for the pure model) was severe with the Metropolis algorithm as could be expected. For example, an interactive run on the $30 \times 30$ lattice with a random hot start within 10% below $T_t$ never seemed to equilibrate in any watchable time. Close to the transition we also examined the autocorrelation time of the magnetization $\tau_M \sim L^z$ and found for relatively small lattice sizes an 'effective exponent' of $z = 2.5$. Of course, for large lattice sizes we expect asymptotically an exponential divergence of $\tau_M$ if the transition is of first order. The cluster algorithm under the same conditions reached equilibration in about 10 minutes on an IBM RISC 320H but gave an 'effective exponent' of $z = 2.1$, not really so much lower. It is something of a puzzle why the latter algorithm behaved so well under simple observation near the transition point, especially since its complexity is $O(N)$ per iteration, the same as the Metropolis. We can only conclude that the kind of large-scale changes that it allows have a much larger effect than the $z$ measurement can encompass, and the designed cluster algorithm certainly passed the most important test of enabling us to complete the calculation within the computer time that we could access.

## 3. Results

Our calculations were made (using periodic boundary conditions) on samples ranging from $30 \times 30$ to $198 \times 198$ on several machines including Sun-SPARC, IBM RISC/6000 320H, 370 and 590 and a Meiko parallel machine with i860 processors. The results presented below are based on detailed analysis of samples $60 \times 60$ and larger, with run times ranging from $10^6$ iterations for the smaller ones to several times $10^5$ for the larger.

The raw data of our simulations are time series of the energy. The evolution plots in figure 2 show our data for the two largest lattices of size $168^2$ and $198^2$. Since we observe a quite pronounced flipping between the ordered and disordered phase already these plots provide quite convincing evidence that the transition is indeed of the first-order type. In the following we shall present a finite-size scaling analysis assuming a first-order transition.

To a given time series of the energy $E = Ve$ we have applied standard reweighting techniques [18] to compute the average energy per site $\langle e \rangle$, the specific heat $C = K^2V(\langle e^2 \rangle - \langle e \rangle^2)$, and the Binder parameter $B = 1 - \langle e^4 \rangle / 3\langle e^2 \rangle^2$ as a function of temperature. Basically the reweighting method relies on the fact that the energy distribution $\mathcal{P}_{K_0}(E)$ (normalized to unit area) at inverse temperature $K_0$ can be written as

$$\mathcal{P}_{K_0}(E) = \Omega(E) \mathrm{e}^{-K_0 E} / Z(K_0) \tag{3.1}$$

with a temperature *independent* density of states $\Omega(E)$. It is then easy to see that an expectation value $\langle f(E) \rangle(K)$ can, in principle, be calculated for any $K$ from

$$\langle f(E) \rangle(K) = \frac{\int_0^\infty \mathrm{d}E \, f(E) \mathcal{P}_{K_0}(E) \mathrm{e}^{-(K-K_0)E}}{\int_0^\infty \mathrm{d}E \, \mathcal{P}_{K_0}(E) \mathrm{e}^{-(K-K_0)E}} . \tag{3.2}$$

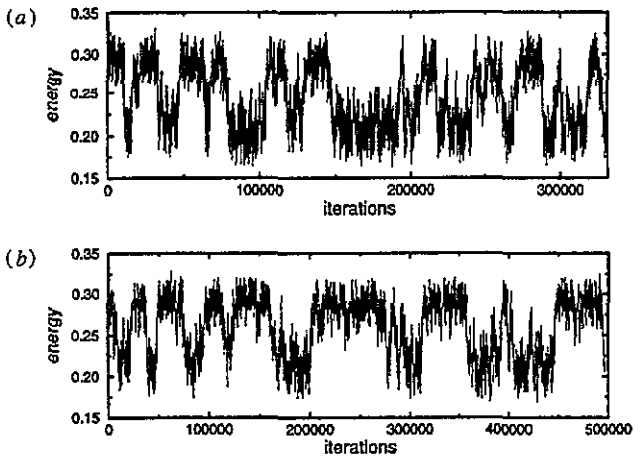


**Figure 2.** Energy time series showing pronounced flips between the ordered and disordered phase. (*a*) $L = 168, T = 0.627\,55$. (*b*) $L = 198, T = 0.6276$.

For discrete energies the integrals have to be replaced by summations, and to keep the notation short we have suppressed the lattice-size dependence of $\mathcal{P}_{K_0}(E)$. In practice, since the wings of $P_{K_0}(E)$ usually have large statistical errors, one expects (3.2) to give reliable results only for $K$ near $K_0$.

In order to avoid bias problems in the reweighted data the error bars are estimated by jack-knife blocking [19] of the time series. This involves dividing the time series into a number $N_B$ of overlapping blocks (each consisting of a fraction $1 - 1/N_B$ of the data), computing the observables for each block separately and then taking the variance over these $N_B$ estimates. In the last step the trivial correlation between the blocks caused by the double counting can be taken into account exactly. For the lattice sizes where we performed several runs at different simulation temperatures we computed error-weighted averages over these runs; see, for example, the discussion by Holm and Janke [20]. The resulting curves together with their error bars for the specific heat and the Binder parameter are shown in figure 3. There is a feature of an apparent shoulder in some of the specific heat data, which often happens when applying (3.2) too far from the simulation point. Despite this it is straightforward to apply the reweighting method to obtain the extrema of these curves with high precision. Again we have estimated the extrema and their statistical errors for each run separately and then applied error-weighted averages to obtain the final values for each lattice size.

### *3.1. Finite-size scaling*

Assuming a first-order phase transition we have tried to fit these data to the asymptotic finite-size scaling ansatz [21]

$$X = a + b/V \tag{3.3}$$

where $X$ stands for the specific-heat maximum $C_{\max}/V$, the Binder-parameter minimum $B_{\min}$, the corresponding locations of these extrema $T_{C_{\max}}$ and $T_{B_{\min}}$, or $C(T_{B_{\min}})$ and $B(T_{C_{\max}})$. As a result we obtain consistent fits with quite acceptable goodness-of-fit parameters $Q$ if we exclude the $L = 60$ and $L = 78$ data. Our estimates of $a$ and $b$ are collected in table 1.

In figure 4 we show the fits to the pseudo-transition temperatures $T_{C_{\max}}$ and $T_{B_{\min}}$. Here the parameter $a$ gives the transition temperature in the infinite volume limit, $a = T_t$. By averaging our two results for $T_t$ we obtain the final estimate

$$T_t = 0.627\,310 \pm 0.000\,058 = 0.627\,31 \pm 0.000\,06 \tag{3.4}$$

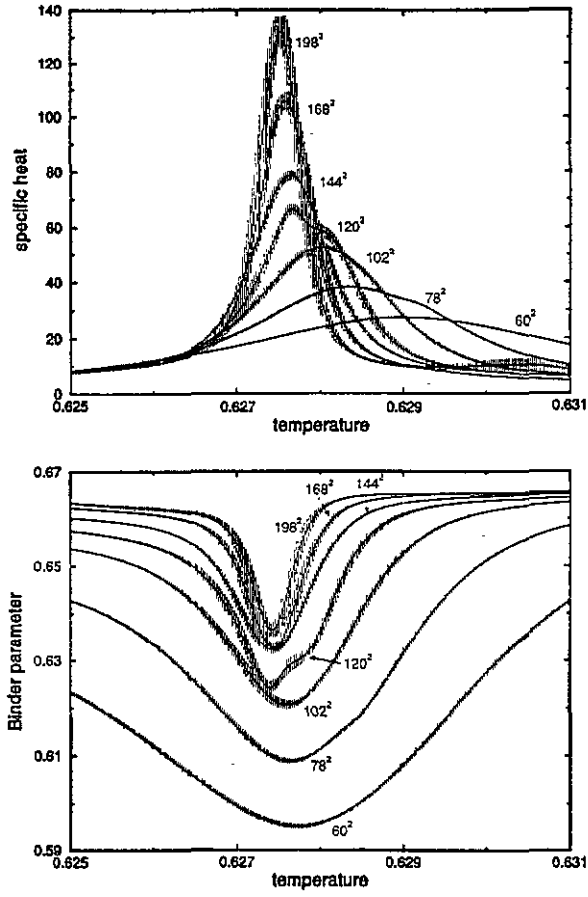


**Figure 3.** The specific heat and Binder parameter as a function of the temperature for various lattice sizes.

**Table 1.** Results of linear least-square fits to the finite-size scaling ansatz $X = a + b/V$, where $X$ denotes the quantities in the first column and $V$ is the lattice volume.

| $X$ | $a$ | $b$ | $\chi^2$/DOF | $Q$ |
|---|---|---|---|---|
| $T_{C_{\max}}$ | 0.627 305(58) | 7.31(99) | 0.37 | 0.78 |
| $T_{B_{\min}}$ | 0.627 314(58) | 2.94(98) | 0.40 | 0.75 |
| $C_{\max}/V$ | 0.002 76(12) | 24.2(1.9) | 1.5 | 0.21 |
| $C(T_{B_{\min}})/V$ | 0.002 60(10) | 19.1(1.5) | 1.5 | 0.21 |
| $B_{\min}$ | 0.641 7(11) | −220(18) | 1.4 | 0.25 |
| $B(T_{C_{\max}})$ | 0.643 1(9) | −175(15) | 1.4 | 0.25 |

which is compatible with, but considerably more accurate than, previous estimates in the literature.

The fits to the data of the specific heat and Binder parameter are shown in figures 5 and 6. Here standard finite-size scaling theory of first-order phase transitions relates the parameter $a$ to the infinite-volume energies in the ordered and disordered phase, $e_o$ and $e_d$. The results for the specific heat are [22, 23]

$$C_{\max}/V = K_t^2 \left(\frac{e_d - e_o}{2}\right)^2 + O(1/V) \tag{3.5}$$

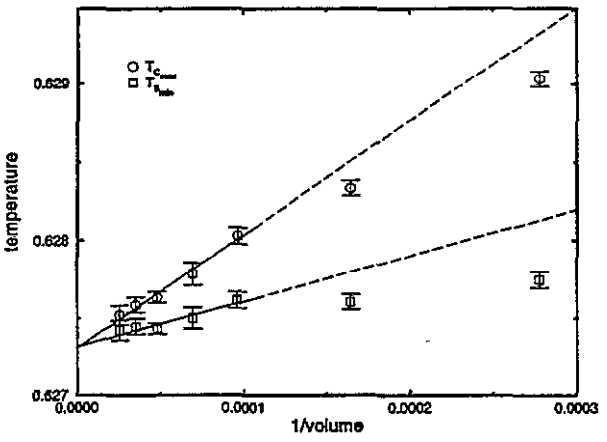


**Figure 4.** Finite-size scaling of $T_{C_{max}}$ and $T_{B_{min}}$.

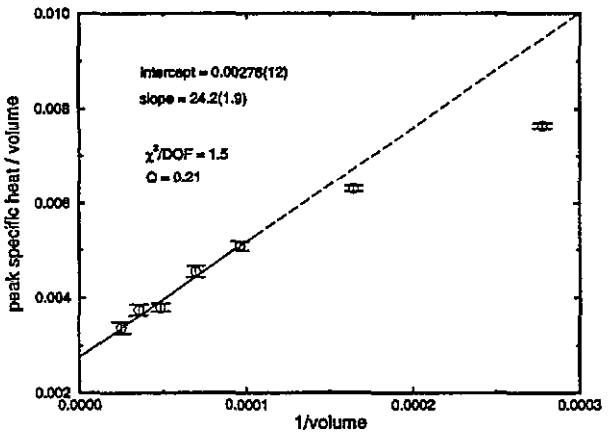


**Figure 5.** Finite-size scaling of $C_{max}/V$.

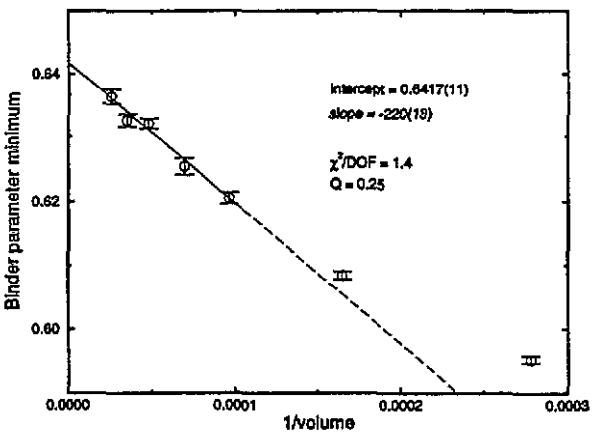


**Figure 6.** Finite-size scaling of $B_{min}$.

and [24]

$$C(T_{B_{min}})/V = K_t^2 \frac{4e_o^2/e_d^2}{(1+e_o^2/e_d^2)^2}\left(\frac{e_d - e_o}{2}\right)^2 + \mathcal{O}(1/V)\,. \tag{3.6}$$

For the Binder parameter one finds [22, 23]

$$B_{\min} = 1 - \frac{1}{12}\left(\frac{e_o}{e_d} + \frac{e_d}{e_o}\right)^2 + \mathcal{O}(1/V) \tag{3.7}$$

and [23]

$$B(T_{C_{\max}}) = 1 - \frac{2}{3}\frac{e_o^4 + e_d^4}{\left(e_o^2 + e_d^2\right)^2} + \mathcal{O}(1/V)\,. \tag{3.8}$$

Solving the equations for $C_{\max}/V$ and $B_{\min}$ for $e_o$ and $e_d$ we obtain

$$\Delta e \equiv e_d - e_o = 2T_t\sqrt{C_{\max}^{(\infty)}/V} \tag{3.9}$$

and

$$e_o = \frac{\Delta e}{2}\left[\sqrt{1 + \frac{2}{\sqrt{3(1 - B_{\min}^{(\infty)}) - 1}}} - 1\right] \tag{3.10}$$

where $C_{\max}^{(\infty)}/V$ and $B_{\min}^{(\infty)}$ denote the infinite volume limits, i.e. the parameter $a$ in table 1. Inserting these numbers in (3.9) and (3.10) we find

$$\begin{aligned} \Delta e &= 0.0659 \pm 0.0015 \\ e_o &= 0.212 \pm 0.011 \\ e_d &= 0.278 \pm 0.012\,. \end{aligned} \tag{3.11}$$

As a check we can now insert the values for $e_o$ and $e_d$ in (3.6) and (3.8), yielding in the infinite volume limit $C(T_{B_{\min}})/V \approx 0.00257$ and $B(T_{C_{\max}}) \approx 0.6433$ in very good agreement with the estimates obtained from the fits in table 1.

### *3.2. Histogram analysis*

As a useful cross-check we have also analysed the energy histograms $P(e)$ which for the quantities considered so far contain almost the same information as the time series (only detailed information about autocorrelation times is lost). Furthermore, they offer an alternative determination of pseudo-transition temperatures whose finite-size scaling behaviour contains no power-law terms [25]. Of course, exponentially small corrections which have always to be added are also visible here. The method [23, 25, 26] consists of first reweighting a given histogram to a temperature $T_{\text{eqh}}$ where both peaks are of equal height. This is usually the case around $T_{C_{\max}}$. The location of the minimum between the two peaks is then used as an energy-cut parameter $e_{\text{cut}}$ which is kept fixed in the next step. Here one further reweights the histogram until at a pseudo-transition temperature $T_{\text{w/w}}$ the weight of the ordered phase, $W_o = \sum_{e<e_{\text{cut}}} P(e)$, equals $\mathcal{N}$ times the weight in the disordered phase, $W_d = \sum_{e>e_{\text{cut}}} P(e)$, where $\mathcal{N}$ is the number of ordered ground states, i.e. in our case $\mathcal{N} = 6$. The typical histogram shapes encountered in this procedure are shown in figure 7 for $L = 168$ and $L = 198$. Even though the transition is only very weakly of first order, we get estimates for $T_{\text{w/w}}$ that are fully consistent with our earlier estimate (3.4), e.g. $T_{\text{w/w}} = 0.627\,230(59)$ for $L = 168$ and $T_{\text{w/w}} = 0.627\,262(65)$ for $L = 198$. The remaining

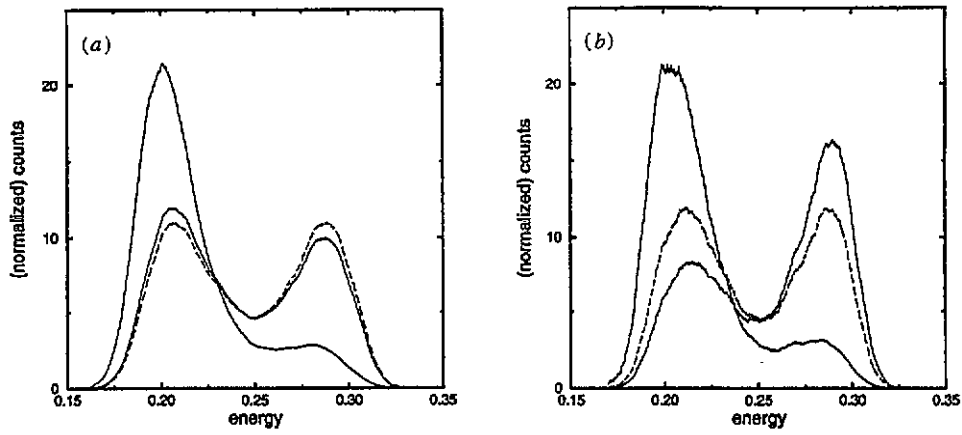


**Figure 7.** Double-peaked input histogram (full curve) reweighted to equal peak height (broken curve) and to a weight ratio 6:1 with the pronounced peak in the ordered phase (full curve). (*a*) $L = 168, T_{\text{run}} = 0.627\,55, T_{\text{eqh}} = 0.627\,581, T_{\text{w/w}} = 0.627\,230$. (*b*) $L = 198, T_{\text{run}} = 0.6276, T_{\text{eqh}} = 0.627\,511, T_{\text{w/w}} = 0.627\,262$.

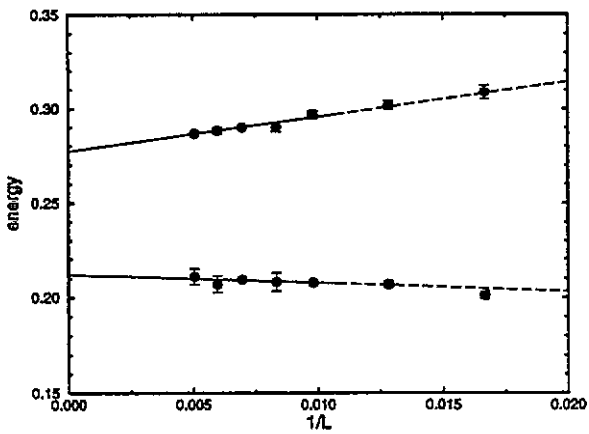


**Figure 8.** Finite-size scaling of the peak maxima of $P(e)$.

small discrepancies with the infinite volume limit should be explainable by exponentially small corrections. Our data are, however, obviously not good enough to allow for such a detailed analysis.

From the equal-height histograms we can read off the positions of the maxima, defining the finite-lattice estimates of $e_o$ and $e_d$ shown in figure 8. The data obviously allow a perfect infinite volume extrapolation in $1/L$. Even though theoretically one expects a cross-over to a $1/V$ behaviour for very large lattice sizes [27], here we used the effectively seen $1/L$ behaviour to obtain from the least-square fits the infinite volume estimates

$$\begin{aligned} e_o &= 0.212 \pm 0.004 \\ e_d &= 0.277 \pm 0.002 \\ \Delta e &= 0.065 \pm 0.005 \end{aligned} \tag{3.12}$$

in extremely good agreement with the values derived from the finite-size scaling of $C_{\max}$ and $B_{\min}$.

Finally, the ratio $P_{\min}/P_{\max}$ of the histogram minimum $P_{\min}$ between the two peaks and the equally high maxima $P_{\max}$ can be used as a finite-lattice definition of the interface tension $\sigma_{od}^{(L)}$ between the ordered (for $e < e_{\text{cut}} \equiv e_{\min}$) and disordered (for $e > e_{\text{cut}}$) phase [28, 29],

$$2\sigma_{od}^{(L)} = \log(P_{\max}/P_{\min})/L\,. \tag{3.13}$$

Here the factor two accounts for the periodic boundary conditions which always enforce an even number of ordered–disordered interfaces. Our results of $2\sigma_{od}^{(L)} = 0.0052(3)$, 0.0059(4), 0.0048(5), 0.0053(7), 0.0037(5), 0.0052(8), 0.0050(7) for $L = 60, 78, 102, 120, 144, 168, 198$ show surprisingly little lattice-size dependence. As the final value we therefore quote the overall mean,

$$2\sigma_{od} = 0.0050 \pm 0.0005 \tag{3.14}$$

where here the error estimate is taken as the variance over the seven lattice sizes.

## 4. Series expansion analysis

We carried out a reanalysis of the Enting–Wu series using the M1 and M2 methods introduced in [14]. To recapitulate our earlier discussion, these have no more reason to work for a first-order transition than do the usual Padé approximants on which they are based, but the precision with which they give critical points for the first-order transitions of the ferromagnetic Potts models is extremely good. We find a very clear indication of good convergence at $u_t = 0.2035 \pm 0.0020$ (or $T_t = 0.628 \pm 0.004$). The relative error is similar to that seen in the ferromagnetic Potts models but the series are shorter. These results confirm the Enting–Wu analyses.

## 5. Conclusions

We have clearly confirmed the first-order nature of the transition, with a method that should be sensitive enough to describe a cross-over to second order if this should occur on dilution. Our final overall result for the transition temperature is in broad agreement with the earlier study of Grest [2] (who only quoted two significant figures) but very much more precise. The other early simulations all claimed three figures of precision that differ from ours in the third figure, but we were unable to deduce error bounds from their papers (thus we cannot comment on whether their values include the precise one). The closest earlier results are those from the series studies (both our reanalysis and the original Enting–Wu numbers) which do include our precise value within their range. This shows (i) that the error estimates on the series values are realistic and (ii) that while an eleven term series is superior to the older small sample simulations, it cannot compete with a precise Monte Carlo study made with the recently developed greatly improved techniques. Both (i) and (ii) are consistent with the picture seen for ferromagnetic $n$-vector models and percolation [30, 31]. Our samples are larger, but not so much larger than those of the simulations of [11], rather we think that it is our superior cluster simulation and histogram analysis methods (and substantially higher statistics) that have enabled us to gain the extra precision. It should be noted that the results of [11] are below all the other calculations and the fact that ours are closer to the central value of the series leads us to believe that our result of $T_t = 0.627\,31 \pm 0.000\,06$ is a reliable and precise evaluation of the critical point for the 3PAFT.

**Acknowledgments**

We thank the GIF (German–Israel Foundation) I-186-097.07/91 for support of visits of WJ to Haifa and JA to Mainz. WJ thanks the Deutsche Forschungsgemeinschaft (DFG) for a Heisenberg fellowship. We also acknowledge the use of the computational facilities of the Technion Minerva Centre for Non-Linear Physics and the Meiko Parallel Computer at the Technion. In addition, AB and SS acknowledge support from GIF, grant no I-131-095.07/89, and from the Israeli Academy of Science and Humanities, grant no 399/90, as well as from the Carl F Gauss Minerva Center for Scientific Computations.

## Appendix. Proof of detailed balance

The statistical validity of the cluster algorithm described in section 2 is a special case of the following well known result due to Kandel and Domany [32]. Replacing the Hamiltonian $H$ by one of the Hamiltonians $H_1, \ldots, H_N$ in probabilities $P_1, \ldots, P_N$, respectively, maintains detailed balance if

$$P_i = q_i e^{\frac{H(S)-H_i(S)}{T}} \qquad i = 1, \ldots, N \tag{A.1}$$

(where $S$ is the configuration at the time of the replacement) provided $q_i$ are independent of $S$, and $\sum_{i=1}^{N} P_i = 1$.

In the case under consideration, it suffices to prove the validity of the basic step of including a new site (for instance, the site $k$ in figure 1($a$)) in a growing cluster. Let $H(S)/T = -K\delta_{s_k,s_i} - K\delta_{s_k,s_j} + H_u/T$, where $H_u$ denotes the terms which remain unchanged upon the site $k$ processing. Then the Hamiltonians $H_1(S)$ and $H_2(S)$ corresponding to the cases of deleting, and freezing, respectively, may be defined as follows:

$$H_1(S) = H_u$$
$$H_2(S) = \infty \cdot \delta_{s_k,s_i} + \infty \cdot \delta_{s_k,s_j} + H_u$$

and it is readily seen that the corresponding probabilities $P_1 = p_d$ and $P_2 = p_f$ (where $p_d$ and $p_f$ are defined by (2.1) and (2.2), respectively) satisfy (A.1) with $q_1 = e^K$, $q_2 = 1 - e^K$.

## References

[1] Schick M and Griffiths R B 1977 *J. Phys. A: Math. Gen.* **10** 2123
[2] Grest G S 1981 *J. Phys. A: Math. Gen.* **14** L217
[3] Saito Y 1982 *J. Phys. A: Math. Gen.* **15** 1885
[4] Enting I G and Wu F Y 1982 *J. Stat. Phys.* **28** 351
[5] Novotny M A and Landau D P 1981 *Phys. Rev.* B **24** 1468
[6] Novotny M A and Evertz H 1993 *Computer Simulation Studies in Condensed Matter Physics* vol VI ed D P Landau, K K Mon and H-B Schüttler (Berlin: Springer) p 188
[7] Binder K and Reger J D 1992 *Adv. Phys.* **41** 547
[8] Adler J, Palmer R G and Meyer H M 1987 *Phys. Rev. Lett.* **58** 882
[9] Adler J, Gefen Y, Schick M and Shih W-H 1987 *J. Phys. A: Math. Gen.* **20** L227
[10] Fried H 1989 *PhD Thesis* University of Washington
[11] Ono I and De Meo M D 1992 *Phys. Rev.* B **46** 12402
[12] Adler J and Privman V 1995 *J. Phys. A: Math. Gen.* **28** 2445
Briggs K M, Enting I G and Guttmann A J 1994 *J. Phys. A: Math. Gen.* **27** 1503
[13] Schreider G and Reger J D 1994 *J. Phys. A: Math. Gen.* **27** 1071
Schreider G 1993 *PhD Thesis* Mainz

[14] Adler J, Chang I and Shapira S 1993 *Int. J. Mod. Phys.* C **4** 1007
[15] *Swendsen R H and Wang J S 1987 Phys. Rev. Lett. 58 86*
[16] Shmulyian S 1993 *MSc Thesis* Weizmann and technical reports
[17] Silverman A and Adler J 1992 *Comput. Phys.* **6** 277
[18] Ferrenberg A M and Swendsen R H 1988 *Phys. Rev. Lett.* **61** 2635; 1989 *Phys. Rev. Lett.* **63** 1658 (erratum)
For related work see, e.g., Falcioni M, Marinari E, Paciello M L, Parisi G and Taglienti B 1982 *Phys. Lett.* **108B** 331
Marinari E 1984 *Nucl. Phys.* B **235** 123
Bhanot G, Black S, Carter P and Salvador R 1987 *Phys. Lett.* **183B** 331
Bowen P B *et al* 1989 *Phys. Rev.* B **40** 7439
Münger E P and Novotny M A 1991 *Phys. Rev.* B **43** 5773
[19] Miller R G 1974 *Biometrika* **61** 1
Efron B 1982 *The Jackknife, the Bootstrap and Other Resampling Plans* (Philadelphia, PA: SIAM)
[20] Holm C and Janke W 1993 *Phys. Rev.* B **48** 936
[21] Borgs C and Kotecky R 1990 *J. Stat. Phys.* **61** 79; 1992 *Phys. Rev. Lett.* **68** 1734
[22] Lee J and Kosterlitz J M 1991 *Phys. Rev.* B **43** 3265
[23] Janke W 1993 *Phys. Rev.* B **47** 14 757
[24] Janke W (unpublished)
[25] Borgs C and Janke W 1992 *Phys. Rev. Lett.* **68** 1738
[26] Janke W 1994 *Computer Simulation Studies in Condensed Matter Physics* vol VII ed by D P Landau, K K Mon and H-B Schüttler (Berlin: Springer) p 29
[27] Bhattacharya T, Lacaze R and Morel A 1995 *Europhys. Lett.* **23** 547 1993; *Nucl. Phys.* B **435** [FS] 526
[28] Binder K 1981 *Phys. Rev.* A **25** 1699 1982; *Z. Phys.* B **43** 119
[29] Janke W, Berg B A and Katoot M 1992 *Nucl. Phys.* B **382** 649
[30] Adler J, Holm C and Janke W 1993 *Physica* **201A** 581
[31] Adler J 1995 *Computer Simulation Studies in Condensed Matter Physics* vol VIII ed D P Landau, K K Mon and H-B Schüttler (Berlin: Springer) to appear
[32] Kandel D and Domany E 1991 *Phys. Rev.* B **43** 8539